Science of the Total Environment 869 (2023) 161817

Contents lists available at ScienceDirect

Science of the Total Environment

journal homepage: www.elsevier.com/locate/scitotenv

Developed compositional source profile and estimated emissions of condensable particulate matter from coal-fired power plants: A case study of Yantai, China

Huanhuan Tong[a,b], Yangjun Wang[a,b,*], Shikang Tao[c], Ling Huang[a,b], Sen Jiang[a,b], Jinting Bian[a,b], Nan Chen[a,b], Manomaiphiboon Kasemsan[d,e], Haiyan Yin[f], Cheng Huang[c], Hui Chen[a,b], Kun Zhang[a,b], Li Li[a,**]

[a] *School of Environmental and Chemical Engineering, Shanghai University, Shanghai 200444, China*
[b] *Key Laboratory of Organic Compound Pollution Control Engineering (MOE), Shanghai University, Shanghai 200444, China*
[c] *Shanghai Academy of Environmental Sciences, Shanghai 200233, China*
[d] *The Joint Graduate School of Energy and Environment, King Mongkut's University of Technology, Thonburi, Bangkok 10140, Thailand*
[e] *Center of Excellence on Energy Technology and Environment, Ministry of Higher Education, Science, Research and Innovation, Bangkok, 10140, Thailand*
[f] *Yantai Environmental Engineering Consulting Design Institute Co., Ltd., Yantai, Shandong 264000, China*

HIGHLIGHTS

- An emission source profile of condensable particulate matter (CPM) was developed.
- This source profile integrated the latest component measurements and activity data.
- CPM emission inventory for coal-fired power plants (CFPPs) was developed.
- Two emission estimation methods of CPM from CFPPs were recommended.

GRAPHICAL ABSTRACT

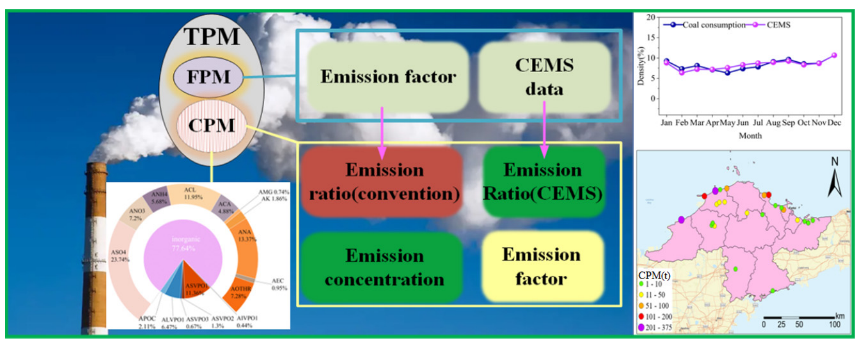

ARTICLE INFO

Editor: Hai Guo

Keywords:
Condensable particulate matter
Emission source profile
Coal-fired power plants
Emission inventory

ABSTRACT

The emission and environmental impact of condensable particulate matter (CPM) from coal-fired power plants (CFPPs) are of increasing concern worldwide. Many studies on the characteristics of CPM emission have been conducted in China, but its source profile remains unclear, and its emission inventory remains high uncertainty. In this work, the latest measurements reported in the latest 33 studies for CPM inorganic and organic species emitted from CFPPs in China were summarized, and then a compositional source profile of CPM for CFPPs was developed for the first time in China, which involved 10 inorganic species and 71 organic species. In addition, the CPM emission inventory of CFPPs in Yantai of China was developed based on surveyed activity data, continuous emission monitoring system (CEMS), and the latest measurement data. The results show that: (1) Inorganic species accounted for 77.64 % of CPM emitted from CFPPs in Yantai, among which SO_4^{2-} had the highest content, accounting for 23.74 % of CPM, followed by Cl^-, accounting for 11.95 %; (2) Organic matter accounted for 22.36 % of CPM, among which alkanes accounted for the largest proportion of organic fraction (72.7 %); (3) Emission concentration method (EC) and CEMS-based emission ratio method ($ER_{FPM,CEMS}$) were recommended to estimate CPM emissions for CFPPs; (4) The estimated CPM emission inventories of Yantai CFPPs in 2020 by the EC method and the $ER_{FPM,CEMS}$ method were 1231 tons and 929 tons, respectively, with uncertainties of −34 % ~ 33 % and −27 % ~ 57 %, respectively;

* Corresponence to: Y. Wang, School of Environmental and Chemical Engineering, Shanghai University, Shanghai 200444, China.
** Corresponding author.
E-mail addresses: yjwang326@shu.edu.cn (Y. Wang), lily@shu.edu.cn (L. Li).

http://dx.doi.org/10.1016/j.scitotenv.2023.161817
Received 22 November 2022; Received in revised form 17 January 2023; Accepted 20 January 2023
Available online 26 January 2023

(5) CPM emissions were mainly distributed in the northern coastal areas of Yantai. This developed CPM source profile and emission inventory can provide basic data for assessing the impacts of CPM on air quality and health. In addition, this study can provide an important methodology for developing CPM emission inventories and CPM emission source profiles for stationary combustion sources in other regions.

1. Introduction

In China, coal is one of the main energy resources (SRWE, 2022), and coal-fired power plants (CFPPs) are one of the important emission sources of air pollution, which emit large amounts of pollutants, such as particulate matter (PM), sulfur dioxide (SO_2), and nitrogen oxides (NO_X) (Wu et al., 2022a). PM emitted from CFPPs can be divided into filterable particulate matter (FPM) and condensable particulate matter (CPM) according to their physical and chemical properties (Wu et al., 2022b). FPM is emitted directly from the stack as solid or liquid phase and can be captured on filter media (Wu et al., 2022a; Yuan et al., 2022b), while CPM is another kind of particulate matter formed by the immediate condensation of gaseous precursors inside the stack as they exit the stack. For example, SO_3, semi- or intermediate volatile organic compounds are gaseous precursors for CPM (Li et al., 2021; Li et al., 2019; Peng et al., 2021; Wang et al., 2020a; Yang et al., 2021; Zhang et al., 2021).

As the earliest proposed CPM measurement method, EPA Method 202 based on the dry impinger method was released (EPA, 2016), which introduced the collection of CPM from condenser, impingers, and CPM filter and recommended placing the condenser vertically to prevent water from collecting in the condenser coils and sample gas from bubbling through it to reduce SO_2 artifact formation. In recent years, many researchers have carried out the measurement of CPM, and some improvements have been made to this method. For example, by comparing with a coil condenser in Method 202, Yuan et al. (2022a) proposed that a chamber condenser can reduce the droplets generation and the contact surface between SO_2 and droplets, thereby reducing the deviation of CPM, especially for high-humidity flue gas. Wang et al. (2020b) conducted a comparative experiment of CPM measurement with the dry impinger method, indirect dilution method, and direct dilution method, and found that the CPM concentration measured by the dry impinger method was significantly overestimated because the impinger solutions absorbed part of the soluble gases (such as SO_2, HCl and NH_3). Moreover, compared to the direct dilution method, the indirect dilution method can better capture the effects of rapid dilution, cooling, and condensation of condensable gaseous precursors in the presence of filterable particulate matter, and the indirect dilution method was accordingly recommended as the appropriate method for the CPM measurement in stationary sources (Wang et al., 2020b). To overcome the shortage of offline CPM monitoring methods, Liu et al. (2022a) developed an automatic online monitoring system by employing the pH and electrical conductivity of CPM solutions. In general, emission measurement methods for CPM and its components have been greatly improved, but even the most reliable indirect dilution method still has large uncertainties. For example, the source of relatively high concentrations of Ca^{2+} still cannot be explained (Wang et al., 2020b). Therefore, accurate measurement of CPM and its chemical composition remains a great challenge.

Since EPA Method 202 was released, many CPM measurements have been reported. For example, CPM emissions accounted for a large proportion of total particulate matter (TPM) (Feng et al., 2018), typically more than 50 % (Li et al., 2017; Lu et al., 2019; Yang et al., 2021; Yuan et al., 2021), and some even exceeding 90 % (Lu et al., 2019; Lu et al., 2020; Wang et al., 2020a; Wu et al., 2021b; Yang et al., 2018; Yang et al., 2015). Its main components are SO_4^{2-} (Li et al., 2017; Lu et al., 2019; Song et al., 2020; Zhai et al., 2022), NO_3^- (Lu et al., 2019; Song et al., 2020), Cl^- (Li et al., 2017; Lu et al., 2019; Song et al., 2020; Zhai et al., 2022), NH_4^+ (Wu et al., 2021a; Zhai et al., 2022; Zheng et al., 2018), semi-volatile organic compounds (SVOCs) (Chen et al., 2022; Liu et al., 2022b; Morino et al., 2018), intermediate volatility organic compounds (IVOCs) (Liu et al., 2022b; Wang et al., 2022) and others. However, except for Wang et al. (2020b) and Zheng et al. (2018), which used the dilution method, most of them employed the US EPA method 202, which has large deviations, as mentioned above. Meanwhile, we noticed that some reported measured CPM contained metal elements (e.g. Fe, Al) (Li et al., 2017; Wu et al., 2020). However, these metal elements cannot be in the gaseous state at the temperature inside the stack, so it is theoretically impossible for CPM to contain them. The main reason for including these metal elements in their measured CPM may be the leakage from FPM during the measurement process. In addition, in recent years, with the implementation of ultra-low emission standards and the continuous improvement of combustion efficiency in order to obtain sufficient economic benefits, China's power plants have very low emissions of organic matter due to high-efficiency combustion (Wang et al., 2020b; Deng et al., 2022). In general, although the measurement method of CPM has been improved, it is still a big challenge to accurately measure the concentrations of CPM and its chemical composition (Wang et al., 2020b), and it is also a challenge to establish an accurate CPM source profile accordingly.

A reliable source profile of CPM emissions from CFPPs is a necessity to accurately evaluate the impact of CPM emissions from CFPPs on air quality. Although some researchers assessed the impact of CFPPs CPM on air quality, they used a source profile of a similar source instead of a CPM source profile, or integrated limited components from published measurements. For example, Li et al. (2022) studied the impact of China's CPM emissions (including that from CFPPs) on organic aerosol OA and $PM_{2.5}$, but the source profile of CFPPs CPM was not shown in their study, and the measurements of CPM components from CFPPs collected by the authors were limited. Furthermore, they did not mention their CPM measurement methods which are closely related to their uncertainties. Morino et al. (2022). Nevertheless, as mentioned above, the CPM measurements of most studies were based on the EPA method 202, which is currently considered to have large deviations. Obviously, low-quality source profile has become one of the main sources of uncertainties in assessing air quality impacts of CFPPs CPM emissions. It is essential to understand the exact species and its proportion to gain better insight into the impact of CPM emissions on air quality. Although the accuracy of the measurement of CPM and its components still needs to be improved, the progress of CPM measurement methods and the increasing abundance of measurement data about the chemical composition of CFPPs CPM emissions make it possible to develop a more comprehensive and reliable CPM source profile of CFFPs. We thereby developed a comprehensive source profile for CFPPs CPM emissions in this study.

Accurate estimation of CPM emissions from stationary combustion sources in a specific city or region is critical for assessing their impact on air quality. Generally, there are three methods for estimating the CPM emission inventory: (1) CPM concentration of emission multiplied by the exhaust gas volume per ton of coal combustion, and then multiplied by coal consumption (EC method for short); (2) multiplying the coal consumption by CPM emission factor (EF method for short); (3) multiplying the FPM emission by the ratio of CPM/FPM (ER method for short). For example, US EPA AP-42 (Fifth Edition): *Compilation of Air Emissions Factors* (EPA, n.d.) provides the EF method for estimating CPM based on ash content and provides 3 emission factors. Wang et al. (2022) applied the EC method and the EF method to estimate China's industrial CPM emissions of 980,000 tons. Morino et al. (2018) estimated OA emissions in CPM from coal-fired sources using the ER method, based on the emission survey data of only one coal-fired source, which showed that OA emission in FPM was 0.01 times that of $PM_{2.5}$, while the total OA emission in FPM and CPM is 0.96 times that of $PM_{2.5}$, with potential high uncertainties. The ER method was also used to estimate the CPM emission of Source Korea by Choi et al. (2019). It is worth noting that the accuracy of CPM estimated by the ER method is highly dependent on the accuracy of the estimated FPM emission. Based on the *Technical Manual for Compilation of Urban Air Pollution Source Emission Inventory* (He, 2018), which is a conventional method recommended by the Chinese government in the past few years, the estimated FPM emissions of CFPPs may be dozens of times that of continuous emission monitoring system (CEMS) data(Chen et al., 2019), indicating that there is a potential big gap between the CPM emissions estimated based on conventional method($ER_{FPM,\ CONV}$) and those estimated based on CEMS($ER_{FPM,\ CEMS}$). However, CPM emissions from CFPPs in China estimated based on different methods have not been assessed.

In this study, we first conducted an on-site survey of activity data for all CFPPs in Yantai, China, and then combined CPM chemical composition measurement data collected from high-quality and latest papers to develop the CPM emission source profile for CFPPs in Yantai. Meanwhile, CPM emission inventories of CFPPs in Yantai were developed, and the uncertainties were analyzed with the Monte Carlo method. In addition, four estimation methods of CPM emission were compared, the main parameters affecting the estimation of CPM emission were discussed, and recommended methods were proposed.

2. Methodology

In this work, a detailed survey of the activity data of all CFPPs in Yantai, China, as shown in Fig. 1, was carried out, and detailed information on 83 units of 25 CFPPs was obtained, including CFPPs types, installed capacity, fuel types, and coal consumption, APCD, stack height and diameter of stack outlet, the exact location of the plant (latitude and longitude), etc. Then, the CPM emission inventory of Yantai CFPPs was developed through a bottom-up approach.

The measurement data used to estimate CPM emission and develop source profile was extracted from 33 previous studies, which involved CPM emission concentration, CPM emission factor, CPM removal efficiency, inorganic and organic components, etc. And the CEMS data from the continuous emission monitoring system of CFPPs in Yantai was obtained to estimate CPM emission and temporal evaluation. The time profile of CPM emission was developed with monthly coal consumptions of CFPPs and hourly CEMS data. The spatial distribution of CPM emission depends on the geographical location information of each CFPPs. Based on these data, the CPM emission source profile and CPM emission inventories of Yantai CFPPs were developed. Moreover, the uncertainty analysis of CPM emission inventories was analyzed with Monte Carlo simulation. Fig. 2 shows a schematic diagram of the study.

2.1. Development of source profile

To develop a more comprehensive and accurate CPM emission source profile and emission inventory, we applied the latest 33 published papers covering the measurements of CPM and its organic and inorganic components. The measurements of inorganic and organic species from those literature were further fused to form CPM source profiles. During this process, we firstly develop the source profile of CPM for CFPPs based on published data of 10 inorganics (including 4 metal ions and 6 nonmetal ions) and 71 organic species. Each measurement of component was extracted from published literature, and quality assessment criteria established by Bray et al. (2019) were used. Several requirements of literature were considered in this study: (1) the installed capacity and APCD reported in literature match well with units in Yantai; (2) the measurement data of chemical compositions from improved methods were used with high priority (3) the measured data of chemical compositions reported in peer-reviewed journal articles were referenced for the profile with high confidence; (4) high priority was given to the published data measured in China. As a result, 33 published papers with inorganic or/and organic species were further fused into CPM source profiles.

We followed the method used by Li et al. (2014) and Sha et al. (2021) to integrate and map species to units after screening the literature. We use data from the improved measurement method in priority, followed by the data measured by Method 202. The improved method mainly followed the studies of Wang et al. (2020b), Yuan et al. (2022a), Shen et al. (2021), Hu et al. (2016), Zheng et al. (2018) and Liu et al. (2022a). If using data extracted from Method 202, the condenser configuration (vertical or inclined), and the location of CPM collection (condenser, impingers and CPM filter) affected whether we used the data. For example, if the measurement method was based on a vertical condenser configuration, and CPM collection included condenser, impingers and CPM filter, then its measurement data was prioritized. An important step is to match the unit properties with those in published papers to obtain inorganic and organic species proportion: (1) We mainly considered the installed capacity and APCD. The species fraction data were preferred to be used if both installed capacity and APCD can be matched in the published papers. The data would be averaged to be used if only installed capacity or APCD can be matched in published papers; (2) If neither installed capacity nor APCD can be matched in published papers, then we used averaged proportion of given species across all available data.

Then we integrate and map these data to each unit: (1) we revise the inorganic fraction by organic fraction (inorganic proportion equal to 1 minus organic proportion), the organic proportion data selected from indirect dilution method in priority. (2) The fraction of each inorganic species was revised using the following Eq. (1). For inorganic and organic species with only one mass profile available, their profiles

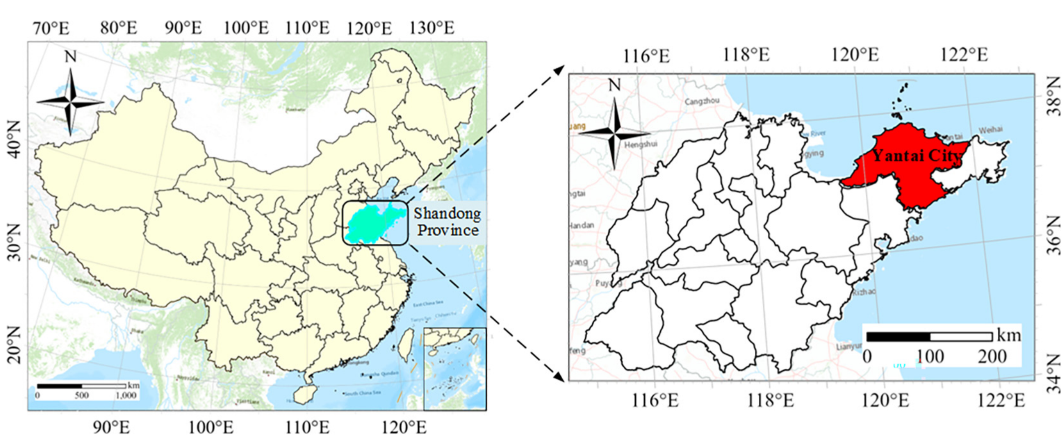

Fig. 1. The location of Yantai, China.

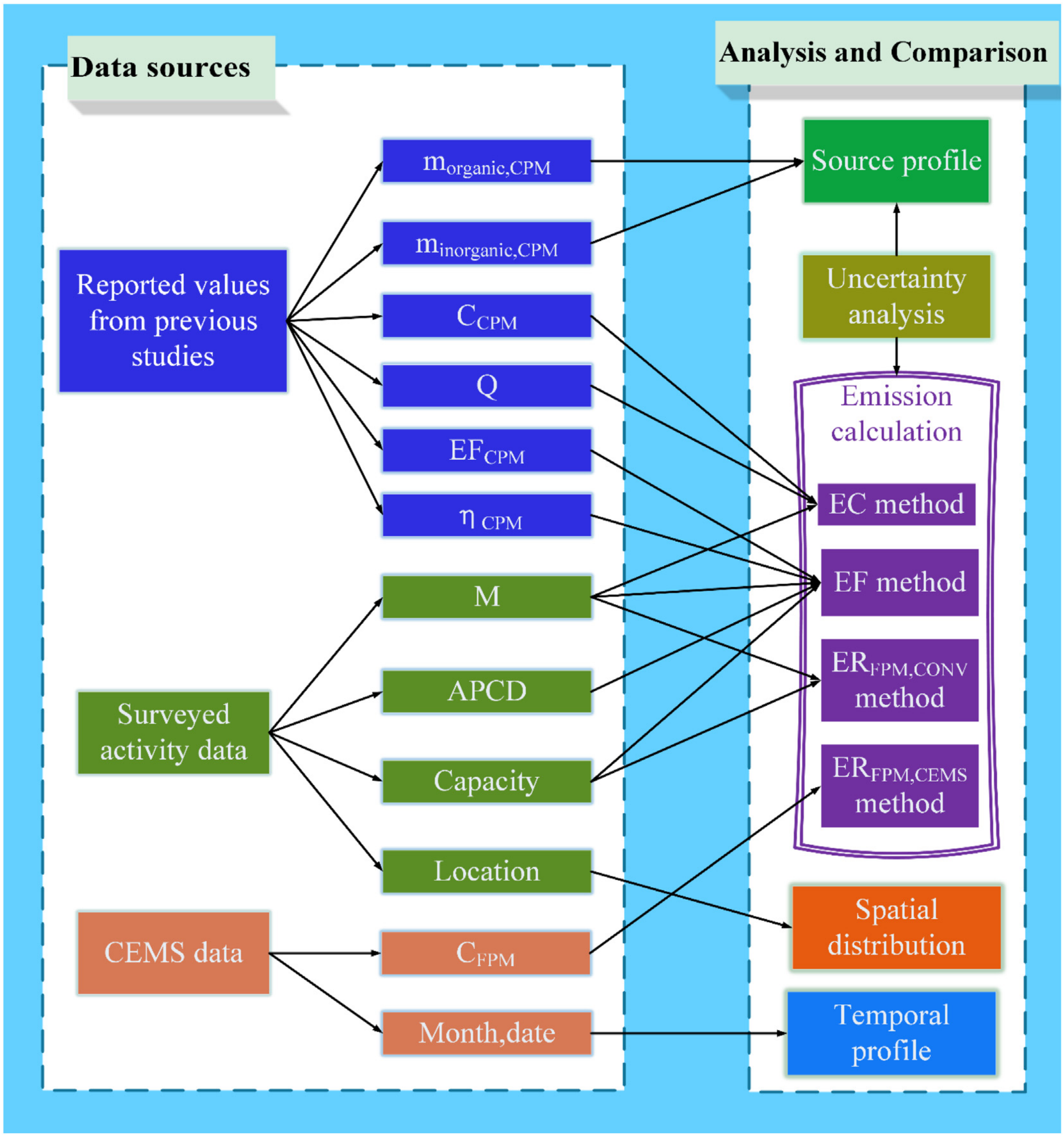

Fig. 2. Schematic diagram of this study.
$m_{inorganic,CPM}$: mass concentration of inorganic species of CPM at the outlet of stack, mg/m^3.
$m_{organic,CPM}$: mass concentration of organic species of CPM at t the outlet of stack, mg/m^3.
C_{CPM}: mass concentration of CPM at t the outlet of stack, mg/m^3.
Q: exhaust volume per ton of coal, m^3/(ton of coal).
EF: CPM emission factor, g/ton (coal).
η:removal efficiency, %.
APCD: air pollution control devices.
M: coal consumption, ton.
Location: include latitude and longitude.
CEMS: continuous emission monitoring system.
C_{FPM}: FPM emission monitoring data from CEMS.

would be fused into one composite profile directly. If there is multiple data of species fraction, it would be averaged using the following Eq. (2).

$$P_{\mathrm{reviced}_{i,j}} = \frac{P_{\mathrm{inorg}_{i,j}}}{\sum_j P_{\mathrm{inorg}_{i,j}}} \times \left(1 - \overline{P}_{\mathrm{org}_i}\right) \tag{1}$$

where $P_{reviced,i,j}$ is the proportion of inorganic species j in the organic-revised inorganic fraction of unit type i; $P_{inorg,i,j}$ is the proportion of inorganic species j in the all of inorganic fraction of unit type i; $\overline{P}_{\mathrm{inorg}_i}$ is the proportion of inorganic species of unit type i.

$$P_{\mathrm{composite}_{i,j}} = \frac{\sum_k P_{\mathrm{i,j,k}}}{K} \tag{2}$$

where $P_{\mathrm{composite}_{i,j}}$ is the proportion of species j in the composite proportion of unit type i; $P_{i,j,k}$ is the original proportion of species j of unit type i; K represents the number of proportions in original data adopted to develop the source profile.

The above process helps establish every species and its proportion in a single unit. The proportion of each species of CPM in all CFPPs of Yantai would be available by weighted summation (weighted by CPM emissions of each unit).

The saturation concentration of each organic species(C^*_i) was estimated based on the number of carbon and oxygens atoms per molecule for the use with the 2-D volatility basis set (VBS) (Pye et al., 2017; Donahue et al., 2011), as shown in Eq. (3).

$$\log_{10} C^*_j = 0.475(25 - n_C) - 2.3n_O + 0.6n_C n_O/(n_C + n_O) \quad (3)$$

where C^*_j is the saturation concentration of organic species j in composite source profile; n_C and n_O are the numbers of carbon and oxygens atoms per molecule, respectively. According to the division criteria proposed by Murphy et al. (2017), organic matter in this study was divided into 7 bins for the Community Multiscale Air Quality Modeling System (CMAQ) simulation.

2.2. CPM emission inventory

In this work, four estimation methods were used to estimate the CPM emissions for CFPPs, which is the emission factor method (EF), the emission concentration method (EC), the emission ratio method based on the CPM/FPM ratio, of which FPM estimated by conventional method ($ER_{FPM,CONV}$), and emission ratio method based on CPM/FPM ratio of which FPM used CEMS data($ER_{FPM,CEMS}$). Table 1 shows the details of these estimation methods.

The removal efficiency of APCD on CPM, CPM concentration, and ratios of CPM/FPM are shown in Fig. S1 Fig. S2, and Fig. S3, the information matching process is similar to that of source profile development, which mainly relies on installed capacity and APCD. The CPM emission factor and exhaust volume per ton of coal combustion are shown in Table S1 and Table S2. Information on those CFPPs such as coal consumption, installed capacity, APCD, etc. was accessed by a survey from key enterprises. The CEMS database contains the online monitoring emission data of key enterprises released by the government based on the same measurement specifications. There are 25 CFPPs in Yantai, but CEMS only provided FPM emission data for 20 CFPPs. The FPM emissions of the remaining 5 CFPPs were estimated based on the FPM emissions obtained by the conventional method and multiplied by the ratio, which is of the CEMS-based FPM emissions of the above 20 CFPPs to their FPM estimated by conventional methods.

2.3. Uncertainty analysis

Uncertainty is an important assessment of the quality of an emissions inventory. A Monte Carlo approach was used to quantify the uncertainty in CPM emissions inventories. By performing Monte Carlo simulations (1,000,000 runs of each probability distribution in this study) on the parameters of interest that introduce uncertainty into CPM emission inventories, upper and lower bounds on CPM emissions of CFPPs within a 95 % confidence interval around the central estimate were evaluated. These parameters involved in uncertainty here are mainly coal consumption, CPM concentration, CPM emission factor, etc., and uncertainty sources in different CPM emission inventory estimate methods are shown in Table S6. The probability distributions of these parameters were determined based on surveys and previous studies from which many data (such as emission ratio of CPM to FPM, etc.) were extracted for this study as described above.

3. Result and discussion

3.1. Activity data

Unit properties, coal consumption, and APCD information are important activity data in this study. The installed capacities of most units are less than 75 MW, accounting for 69 % of the total number of units in Yantai, followed by units with installed capacities of 110-670 MW, accounting for 26 %; other units have installed capacities of 1000 and 1050 MW, accounting for 5 %. There were 24,739,204 tons of coal consumption in 2020, which is dominated by raw coal, followed by bituminous and lignite. We also summarized the APCD data of CFPPs. The majority of preliminary dedust devices were electrostatic precipitators (ESP), electrostatic-bag-precipitator (EBP) and fabric filters(FF). Wet flue gas desulfurization (WFGD) accounts for the majority of desulfurized devices, with gypsum being the most widely used slurry, followed by ammonia and magnesium oxide. All units use low NOx combustion technology to decrease NOx emission, and most units are equipped with selective catalytic reduction (SCR) or selective noncatalytic reduction (SNCR) devices for denitration. WESP is the most popular deep dedust device installed in CFPPs, and most units in the previous studies reporting CPM measurements have a wet electrostatic precipitator (WESP) installed, which makes it reasonable for us to use some of their data.

3.2. Source profile

Fig. 3 shows the source profile of CPM of CFPPs in Yantai, which was developed by integrating the measured data of CPM and its components in previous studies (Table S3, Table S4 and Table S5), and the CFPPs activity data in Yantai. We integrated all species of CPM and mapping into units, as a result, the CPM species of each unit was composited of the summarized species from several studies. Considering the strong influence of unit type, APCD type, etc. on the component proportions in CPM, we mapped and revised these component proportions from previous studies

Table 1
CPM emission estimation methods.

Method	Explanation	Equations
EF	CPM emission is equal to the CPM emission factor multiplied by coal consumption and CPM emission rate, which is equal to 1 minus the CPM removal efficiency.	$CPM_{m,n} = M \times EF_{m,n} \times (1 - \eta_{CPM,n})/10^6$ Where m represent installed capacity, MW; n represents APCD of CFPP; $CPM_{m,n}$ is CPM emission of the unit, ton; M is coal consumption, ton; $EF_{m,n}$ is CPM emission factor, g/ton. $\eta_{CPM,n}$ is CPM removal efficiency of APCD on CPM,%.
EC	This method is based on the emission concentration of CPM, the exhaust gas volume flow per ton of coal burned, and the coal consumption (Chen et al., 2022).	$CPM_{m,n} = A_{CPM,m,n} \times Q \times M/10^9$ Where $A_{CPM,m,n}$ is CPM concentration in the plume, mg/m^3; Q is exhaust volume per ton of coal combustion, m^3/ton.
$ER_{FPM,CONV}$	CPM emission is equal to FPM emission multiplied by the CPM/FPM ratio reported in previous studies. FPM emission is estimated based on the conventional method according to the *Technical Manual for Compilation of Urban Air Pollution Source Emission Inventory*.	$E_{FPM,CONV} = M \times Aar \times w_m \times (1 - \eta_{FPM,n})$ Where $E_{FPM,CONV}$ is FPM emission, ton; Aar is the ash content of coal as burned, %; w_m is the conversion coefficient of ash to FPM, %; $\eta_{FPM,n}$is FPM removal efficiency of APCD,%. $CPM_{m,n,CONV} = E_{FPM,CONV} \times \frac{A_{CPM,m,n}}{A_{FPM,m,n}}$ Where $\frac{A_{CPM,m,n}}{A_{FPM,m,n}}$ is the ratio of CPM/FPM of units extracted from previous studies.
$ER_{FPM,CEMS}$	CPM emission is equal to FPM emission multiplied by the CPM/FPM ratio reported in previous studies. Here, the $PM_{2.5}$ emission was acquired from CEMS data.	$CPM_{m,n,CEMS} = E_{FPM,CEMS} \times \frac{A_{CPM,m,n}}{A_{FPM,m,n}}$ Where $E_{FPM,CEMS}$ is FPM emission based on CEMS data, ton.

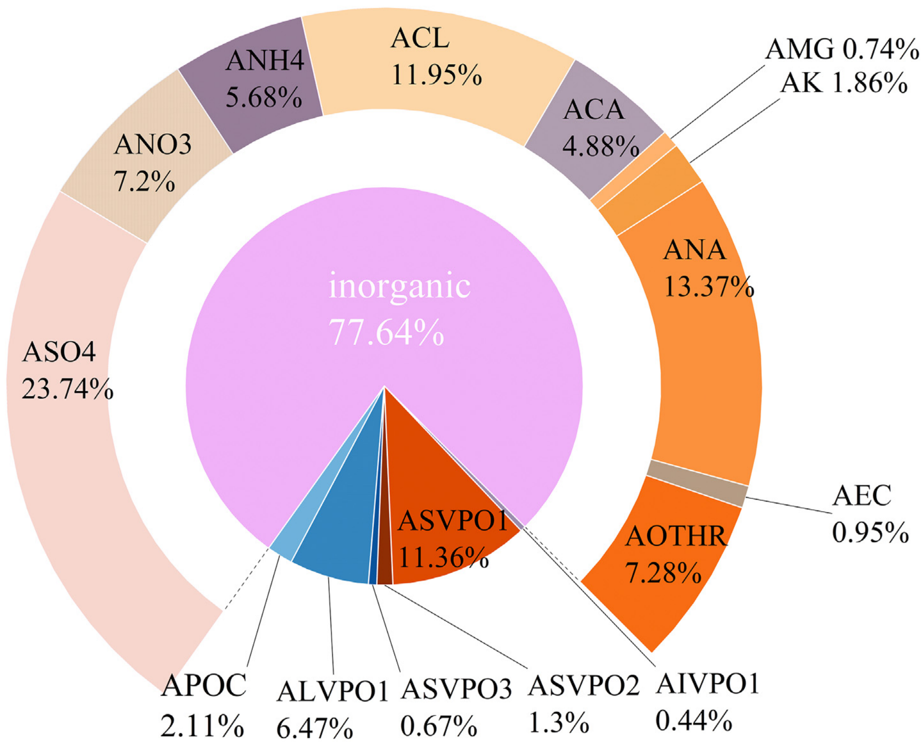

Fig. 3. Source profile of CPM emitted from the CFPPs. The abbreviations are from the chemical mechanism of cb6r3_ae7_aq in the CMAQ model (EPA, 2020).

to each unit in Yantai. For example, the proportions of SO_4^{2-} in different units vary from 4 % to 45 %, with an average of 12 %, as shown in Fig. S4a. Multiply the CPM emission of each unit (1231.4 tons in total) by the proportions of SO_4^{2-} of each unit, all the units emitted 302.71 tons of SO_4^{2-} in total, and proportion of SO_4^{2-} in the CPM emitted by the Yantai units is 23.74 % as a result. We conducted this process for every inorganic and organic species for the source profile.

Compared with organic components, inorganic components have fewer species and are easier to measure, so there are many studies on the measurement of inorganic components, allowing us to obtain abundant data to form the inorganic section of the CPM source profile. Fig. S4b shows the measured data of the inorganic components in CPM reported in the literature, which account for 40–60 % of the CPM, and the proportion of inorganic components does not change significantly with the installed capacity. It should be noted that most of the data of Fig. S4b were measured by Method 202, which overestimated the mass contribution of organic components. As the installed capacity increases, the proportion of inorganic components is expected to rise, usually due to the higher combustion efficiency in larger units, and a lower proportion of organic components in CPM indicates a higher proportion of inorganic components in CPM. This data comes from different studies and may fluctuate due to differences in measurement methods, coal quality, and unit status. Fig. 3 shows that the inorganic components account for 77.64 % of the weighted average of CPM emission, which is lower than the proportion in some literature. This is because the previous studies reported that inorganic content accounted for over 85 % of the majority of CPM (Deng et al., 2022). In the inorganic fraction of the CPM profile, SO_4^{2-} is the highest proportion of inorganic components, accounting for 23.74 % of CPM. The proportion of SO_4^{2-} in the inorganic species is comparable to the measurements of Wang et al. (2020a), Song et al. (2020), Wu et al. (2021a), and Zhai et al. (2022). SO_4^{2-} accounted for 30.58 % of the inorganic fraction, which is lower than that in plumes (more than 60 %) (Ding et al., 2021), because in-cloud oxidation of SO_2 is the key for the fast formation of the total sulfate budget. NH_4^+ is the only cation among the nonmetal ions, accounting for 5.68 % of CPM, it may be explained that a large amount of NH_3 is introduced during the SCR denitration process, especially more ammonia reacts with acid gas to form ammonium compounds, including $(NH_4)_2SO_4$, NH_4HSO_4 and NH_4Cl in the ammonia escape event (Li et al., 2021; Peng et al., 2021; Yang et al., 2021; Yang et al., 2022). Na^+ is the metal ion with the highest content in CPM, with a proportion of 13.37 %. It can exist in coal in the form of mineral sodium, water-soluble sodium, and organic sodium. During combustion, the Na atoms are brought to the surface of the coal particles with moisture and then evaporate with increasing temperature. These atoms then react with oxygen to form Na_2O, and further interact with SO_2, P_4O_6, and HCl to form Na_2SO_4, Na_3PO_4, and NaCl with silicate or chlorate, respectively. Once condensed, these substances form sub-micrometer particles that are easily soluble in water, thus becoming Na^+ (Zheng et al., 2018).

Fig. 3 also shows that organic matter accounts for 22.36 % of the CPM, which is comparable to the measurements of Li et al. (2017), Wang et al.

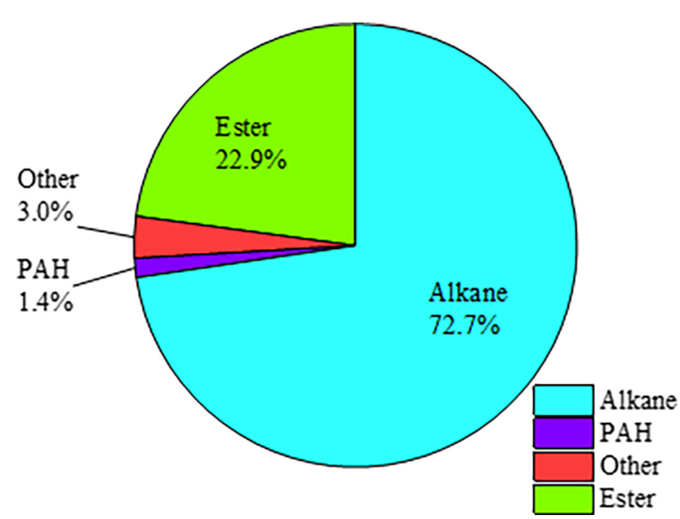

Fig. 4. The proportion of each component in the organic matter of CPM.

(2020a), and Song et al. (2020). As shown in Fig. 4, alkane was the most abundant species (72.7 %) in organic matter, followed by esters (22.9 %), PAH (1.4 %), and others (3.0 %). Generally, compared with inorganic species, we cannot obtain a large number of measurement data of organic species from published papers due to the difficulty of measurement. Moreover, the relatively large amount of species obtained in published papers was divided into 6 bins based on the VBS classification method. Semi-volatile organic compounds and intermediate volatility organic compounds are the main components in CPM organic matter.

The proportions of inorganic components including metal ions and nonmetal ions in the CPM are shown in Fig. 5(a) and Fig. 5(b). Regarding the relationship between inorganic fraction and installed capacity, it indicated that the inorganic substances are dominated by nonmetal ions, and as the installed capacity increases, the proportion of metal ions increases. Fig. 4(b) shows that by comparing the metal ions and nonmetal ions of different APCDs, the units installed with LLT-ESP correspond to a higher proportion of metal ions. On the contrary, the proportion of nonmetal ions corresponding to the unit of bag filter or electrostatic bag filter is relatively high.

Fig. S5 shows the source profile of units with different installed capacities and APCD, we classified the units with an installed capacity of less and over 300 MW and whether installed deep dedust devices. It indicates that there are great differences between inorganic and organic components with the change of installed capacity, and SO_4^{2-} is the major change of inorganic species and semi-volatile organic compounds are the major changes of organic components. Moreover, with the increase of installed capacity, the proportion of inorganic components increases significantly, which is because the proportion of organic components is lower in large CFPPs with higher combustion efficiency. Low volatile and semi-volatile compounds have a higher proportion in the CPM of units with lower installed capacity, which is affected by coal type, combustion technology, combustion temperature, and APCD, etc. (Zhang et al., 2021).

3.3. CPM emissions

The estimated CPM emissions of Yantai CFPPs based on the four methods (EC, EF, $ER_{FPM\text{-}CEMS}$, and $ER_{FPM,CONV}$) are 1231, 2111, 929, and 58,784 tons, respectively, and the FPM emissions based on CEMS and conventional method are 391 tons and 21,062 tons, respectively, as shown in Fig. 6.

The CPM emission calculated by the $ER_{FPM,CONV}$ method was significantly higher than that calculated by the other methods, mainly due to the large FPM emissions of CFPPs, which was estimated based on the conventional method with highly overestimated emission factor of FPM from the *Technical Manual for Compilation of Urban Air Pollution Source Emission Inventory* issued by the government. The same problem was pointed out in another study (Chen et al., 2019). It should be noticed that the FPM emission based on the conventional method is 53.9 times larger than that of CEMS, which is larger than that of Chen's, probably because of the implementation of ultralow emission (ULE) standards in CFPPs and advanced APCD used in China. In addition, the guidance on the emission factors for the conventional estimation of FPM emissions was published before implementing the ULE standard. Consequently, the CPM emission estimated by $ER_{FPM,CONV}$ is indirectly one or two times higher than that of $ER_{FPM,\ CEMS}$. Therefore, the method of $ER_{FPM\text{-}CEMS}$ is more reliable than that of $ER_{FPM,CONV}$ in the estimation of CPM emissions. However, there was no such significant difference among CPM emissions based on EC, EF, $ER_{FPM\text{-}CEMS}$, mainly because CPM and FPM were emitted simultaneously from the stack, and the measurement data of CPM concentration, FPM concentration, and the ratio of CPM/FPM used in EC, EF, $ER_{FPM\text{-}CEMS}$ methods were obtained from previous studies which were carried out after the implementation of the ULE standard. It is worth noting that, the CPM emission factor in the EF method was calculated based on measured CPM concentration (Yuan et al., 2022b), providing high confidence for CPM emission estimation. On the contrary, the measurement data of emission factor for the EF method is relatively insufficient leading to relatively large uncertainties in the estimation of CPM emission based on the EF method.

3.4. Spatial and temporal distributions

3.4.1. Spatial variation

The spatial distributions of CPM emissions from CFPPs of Yantai estimated based on the four methods are shown in Fig. 7. Obviously, the spatial distribution of CPM emissions estimated based on the EC method is similar

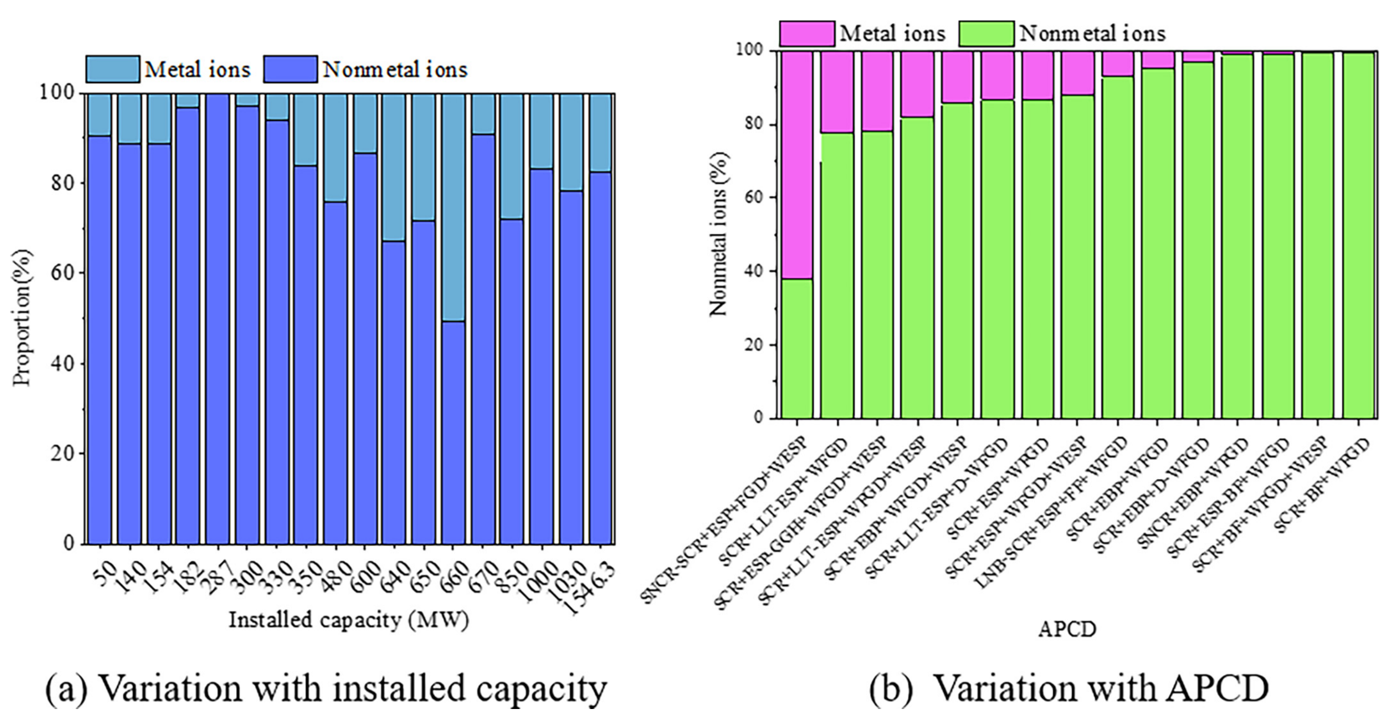

Fig. 5. The proportions of metal ions and nonmetal ions in the inorganic fraction of CPM emitted from CFPPs.

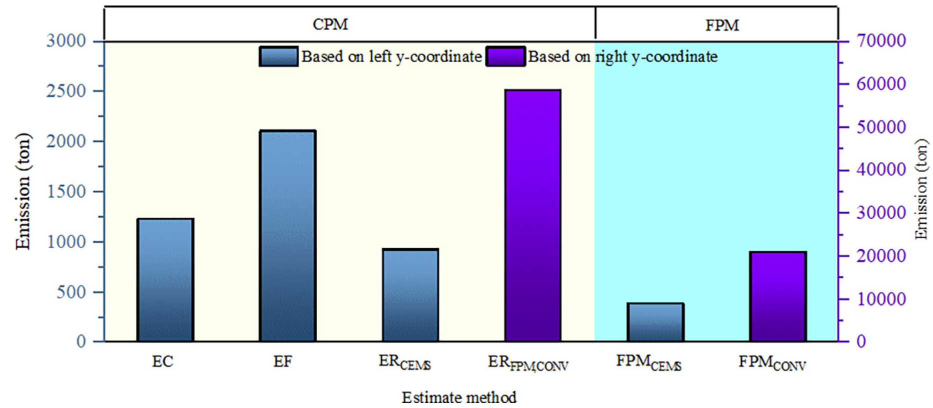

Fig. 6. CPM and FPM emissions of CFPPs based on different estimated methods. The area filled with yellow represents CPM emission, and the area filled with cyan represents FPM. The EC, EF, ER_{CEMS}, $ER_{FPM,CONV}$ represent the emission concentration method, the emission factor method, the emission ratio method based on CEMS and the conventional method for estimation of CPM emission, respectively.

to that of $ER_{FPM,CEMS}$ method, indicating that the CFPPs with large emissions are in the northern part of Yantai. However, it is easy to notice that there are several CFPPs whose CPM emissions based on the EF method were significantly larger than those of the EC method and ER_{CEMS} method, in which there is no significant difference between those for the EC method and the ER_{CEMS} method. Generally, the total CPM emission estimated based on of the EF method was greater than those of the EC and $ER_{FPM,CEMS}$ methods.

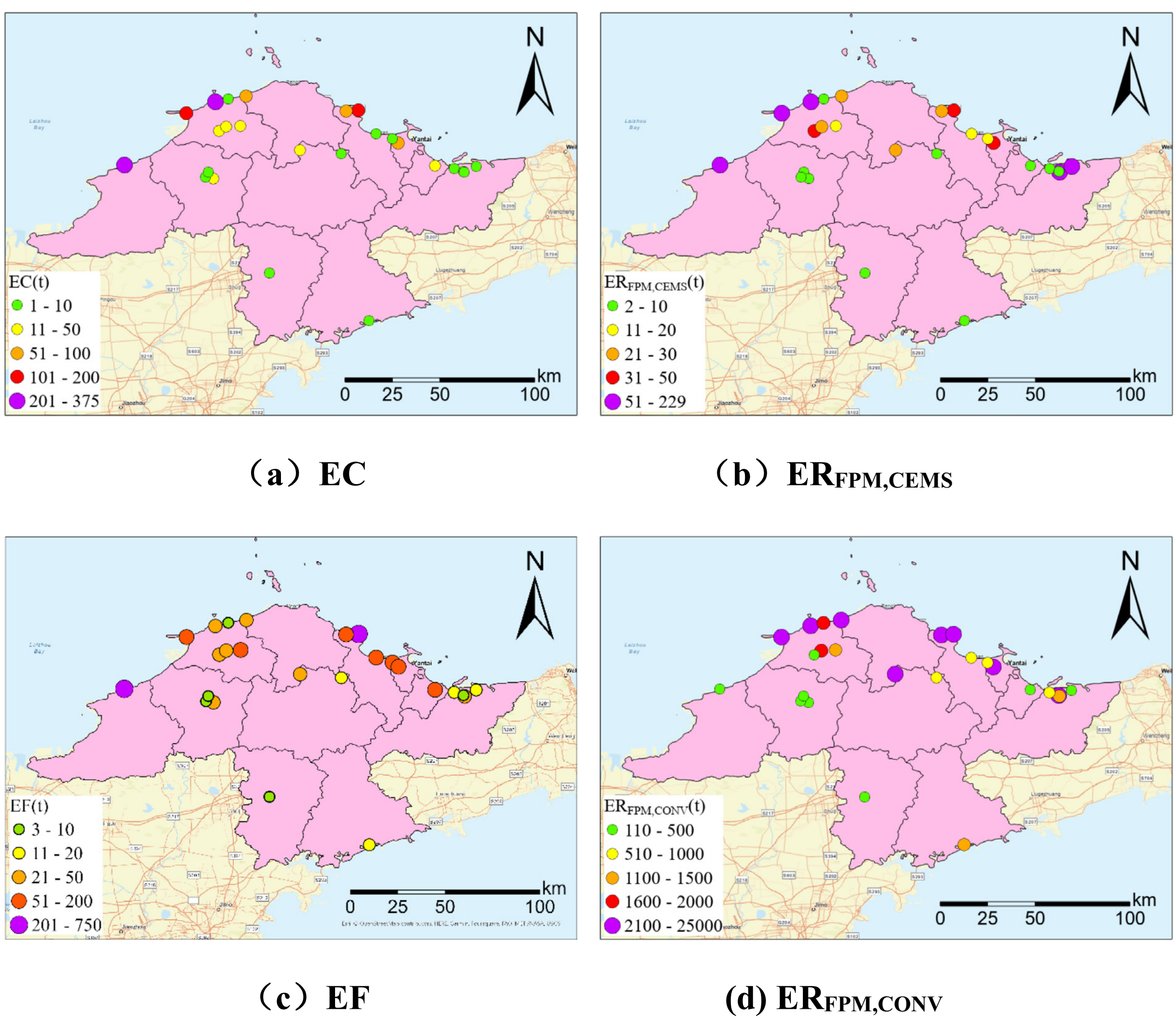

Fig. 7. Spatial distributions of CPM emissions estimatedby the different methods.

3.4.2. Temporal variation

For CFPPs, the temporal patterns of CPM emissions generally depend on fuel consumption (Pham et al., 2008), and this is also true in China (Chen et al., 2019). Fig. 8 Temporal profile(a) shows two close lines for monthly emission fractions based on coal consumption and CEMS data, respectively. Emissions were more in winter. For example, CPM emissions in December accounted for about 10.7 % of the total annual CPM emissions, which was significantly higher than that in summer, mainly because residents' responsibility for heating in winter led to an increase in coal consumption in CFPPs. Fig. 8 Temporal profile(a) shows a lower proportion of emissions in February, mainly due to lower industrial electricity demand during the COVID-19 lockdown. Monthly emissions percentages continued to increase from May to September as industrial, and living activities gradually returned to normal. Fig. 8 Temporal profile(b) shows the weekly variation of CPM emissions. Obviously, emissions were more in the middle of the week (i.e., Tuesday to Friday) with a unimodal distribution and relatively lower emissions on Sunday. The emissions on Wednesday and Thursday accounted for larger proportions of 14.6 % and 14.7 %, respectively, implying that the temporal variation of CPM emissions was highly related to anthropogenic activities.

3.5. Uncertainty analysis

The probability distributions of CPM emissions are shown in Fig. 9, with more details in Table S7. The confidence levels of EC and $ER_{FPM,CEMS}$ methods are −34 % to 33 % and −27 % to 57 %, respectively. The Monte Carlo simulation on CPM emission based on the EC method was the closest to the estimated value. The EF method overestimates 0 to 175 % and $ER_{FPM,CONV}$ method shows uncertainties with −43 % to 45 %. Obviously, both EF and $ER_{FPM,\ CONV}$ methods do have larger uncertainty. The main uncertainties came from factors of exhaust gas volume per ton of coal combustion, CPM concentration, CPM emission factor, CPM removal efficiency of APCD, conventional FPM emission factor, and CPM/FPM ratio. Uncertainties were also affected by the abundance of each estimated parameter as some missing information was replaced by similar or average parameters of the units. In short, EC and $ER_{FPM,CEMS}$ methods are recommended for estimating CPM emissions from CFPPs due to lower uncertainties. This newly established comprehensive CPM emission inventory provides more reliable input data for atmospheric modeling and future decision-making for $PM_{2.5}$ pollution mitigation.

The uncertainty of the CPM emission source profile mainly came from the measurement deviations of the measurement data in the literature, the richness of the measured components of CPM, and the deviations caused by the data mapping during the process of developing the CPM emission source profile. In this study, Yantai was taken as an example city to develop the CPM emission source profile, so if this source profile is used as the CPM emission source profile of other regions, there will be additional uncertainties due to regional differences. Admittedly, this study provides an important methodology for developing CPM emission inventories and CPM emission source profiles for stationary combustion sources in other regions.

4. Conclusion

In recent years, the CPM emissions of CFPPs and their impact on the atmospheric environment have attracted more and more attention, but there are still no reliable CPM emission source profile and emission inventory for CFPPs. In this work, an integrated compositional CPM emission source profile of CFPPs based on the abundant and up-to-date measurement data was developed for the first time, and this integrated compositional source profile would help support the development of speciated emission inventory of CPM and air quality modeling. This source profile includes 10 inorganic species and 71 organic species, of which the inorganic species mainly include 6 nonmetal ions and 4 metal ions, and the organic species mainly include alkanes, esters, PAHs, and others. The inorganic species accounted for 77.64 % of CPM, among which SO_4^{2-} accounted for the highest proportion (23.74 % in CPM), followed by Cl^- (11.95 % in CPM). The organic species accounted for 22.36 % of CPM, of which alkanes accounted for 72.7 % of organic fractions, followed by esters, which accounted for 22.9 % of organic fractions. The time profile of these CPM emissions is based on the time pattern of FPM emissions coming from CEMS data of CFPPs. For CFPPs in Yantai of China, the units with higher CPM emissions are located on the northern coastline of Yantai.

Based on the on-site survey of activity data of CFPPs and emission-related parameters, a bottom-up approach was adopted to develop the Yantai CFPPs' 2020 CPM emissions inventory. By comparing four estimation methods of CPM emissions, the EC and $ER_{FPM,CEMS}$ methods were recommended for estimating CPM emissions due to their low uncertainties. Based on EC and $ER_{FPM,CEMS}$ methods, the estimated CPM emissions of CFPPs in Yantai of China in 2020 are 1231 tons and 929 tons, respectively, and the corresponding uncertainties based on Monte Carlo simulations were −34 % ~ 33 % and −27 % ~ 57 %, respectively.

The source profile of CPM emission and the emission inventory from CFPPs were developed by taking Yantai as an example city, so there will be additional uncertainties due to regional differences if they are used for other regions. Nevertheless, this study provides an important methodology for developing CPM emission inventories and CPM emission source profiles for stationary combustion sources in other regions.

CRediT authorship contribution statement

Huanhuan Tong: Writing – original draft, Methodology, Data curation, Validation, Formal analysis. **Yangjun Wang:** Conceptualization, Writing – original draft, Methodology, Validation, Formal analysis. **Shikang Tao:**

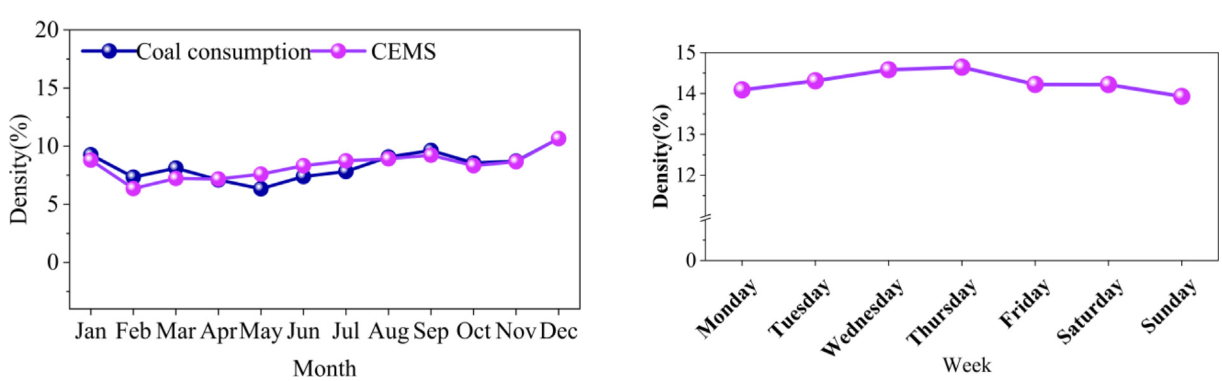

(a) Monthly (b) Day-of-week

Fig. 8. Temporal profiles of CPM emissions.

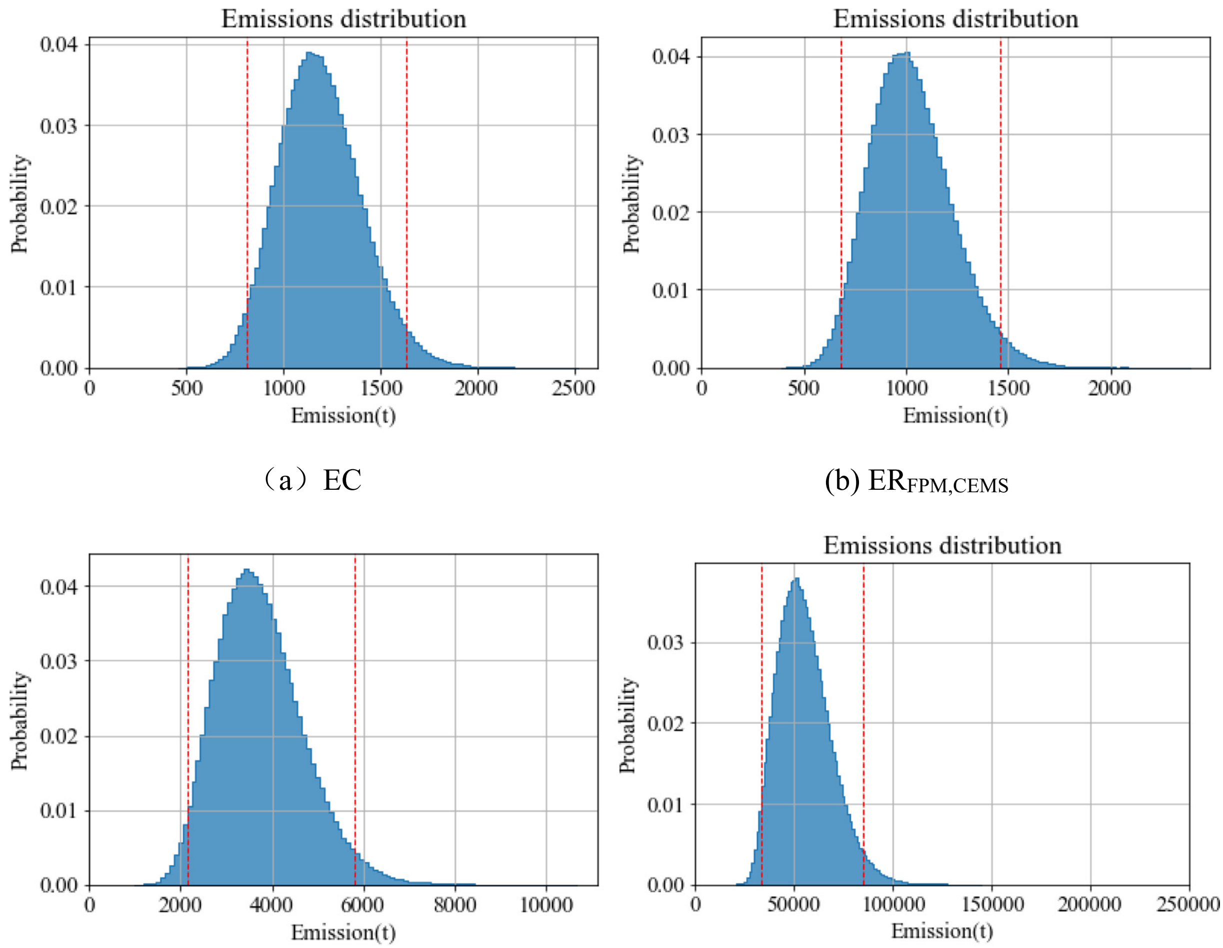

(a) EC

(b) $ER_{FPM,CEMS}$

(c)EF

(d) $ER_{FPM, CONV}$

Fig. 9. Uncertainties in CPM emissions estimated by different methods. The dashed red lines correspond to the 95% confidence intervals.

Writing – review & editing. **Ling Huang:** Writing – review & editing. **Sen Jiang:** Visualization. **Jinting Bian:** Visualization. **Nan Chen:** Visualization. **Manomaiphiboon Kasemsan:** Methodology. **Haiyan Yin:** Data curation. **Cheng Huang:** Writing – review & editing. **Hui Chen:** Writing – review & editing. **Kun Zhang:** Writing – review & editing. **Li Li:** Conceptualization, Methodology, Writing – review & editing.

Data availability

Data will be made available on request.

Declaration of competing interest

The authors declare that they have no known competing financial interests or personal relationships that could have appeared to influence the work reported in this paper.

Acknowledgements

This study was financially supported by the National Natural Science Foundation of China (42075144, 42005112), Open Foundation of State Environmental Protection Key Laboratory of Sources and Control of Air Pollution Complex (No. SCAPC202003), and the Shanghai International Science and Technology Cooperation Fund (NO. 19230742500).

Appendix A. Supplementary data

Supplementary data to this article can be found online at https://doi.org/10.1016/j.scitotenv.2023.161817.

References

Bray, C.D., Strum, M., Simon, H., Riddick, L., Kosusko, M., Menetrez, M., et al., 2019. An assessment of important SPECIATE profiles in the EPA emissions modeling platform and current data gaps. Atmos Environ 207 (1994), 93–104.

Chen, X., Liu, Q., Sheng, T., Li, F., Xu, Z., Han, D., et al., 2019. A high temporal-spatial emission inventory and updated emission factors for coal-fired power plants in Shanghai China. Sci Total Environ. 688, 94–102.

Chen, T.W., Chen, J., Liu, Z., Chi, K., Chang, M., 2022. Characteristics of PM and PAHs emitted from a coal-fired boiler and the efficiencies of its air pollution control devices. J. Air Waste Manag. Assoc. 72, 85–97.

Choi, D.S., Kim, Y.M., Lee, I.H., Jeon, K.J., Choi, B.J., Park, Y.K., 2019. Study on the contribution ratios of particulate matter emissions in differential provinces concerning condensable particulate matter. Energ. Environ. 30 (7), 1206–1218.

Deng, J., Wanng, D., Liu, T., Li, X., Yang, S., Duan, L., Jiang, J., 2022. Organic components in condensable particle matter emitted from coal-fired power plants and steel plants. Environmental engineering 40 (2), 13–17.

Ding, X., Li, Q., Wu, D., Wang, X., Li, M., Wang, T., et al., 2021. Direct observation of sulfate explosive growth in wet plumes emitted from typical coal-fired stationary sources. Geophys. Res. Lett. 48 (6), e2020GL092071.

Donahue, N.M., Epstein, S.A., Pandis, S.N., Robinson, A.L., 2011. A two-dimensional volatility basis set: 1. organic-aerosol mixing thermodynamics. Atmos. Chem. Phys. 11, 3303–3318.

Feng, Y., Li, Y., Cui, L., 2018. Critical review of condensable particulate matter. Fuel 224, 801–813.

He, K.B., 2018. Technical Manual for Compilation of Urban Air Pollution Source Emission Inventory [M]. Tsinghua University. (in Chinese).
Hu, Y., Feng, Y., Wang, S., Ma, Z., Jiang, T., 2016. Studies on monitoring method of condensable particulate and water-soluble ions in fumes from coal fired boilers. Adm. Technol. Environ. Monit. 28, 41–45 (in Chinese).
Li, M., Zhang, Q., Streets, D., He, K., Cheng, Y., Emmons, L., et al., 2014. Mapping asian anthropogenic emissions of non-methane volatile organic compounds to multiple chemical mechanisms. Atmos. Chem. Phys. 14, 5617–5638.
Li, J., Qi, Z., Li, M., Wu, D., Zhou, C., Lu, S., et al., 2017. Physical and chemical characteristics of condensable particulate matter from an ultralow-emission coal-fired power plant. Energy Fuel 31, 1778–1785.
Li, X., Zhou, C., Li, J., Lu, S., Yan, J., 2019. Distribution and emission characteristics of filterable and condensable particulate matter before and after a low-low temperature electrostatic precipitator. Environ. Sci. Pollut. Res. Int. 26, 12798–12806.
Li, J., Li, X., Wang, W., Wang, X., Lu, S., Sun, J., et al., 2021. Investigation on removal effects and condensation characteristics of condensable particulate matter: field test and experimental study. Sci. Total Environ. 783, 146985.
Li, M., Yu, S., Chen, X., Li, Z., Zhang, Y., Song, Z., Liu, W., et al., 2022. Impacts of condensable particulate matter on atmospheric organic aerosols and fine particulate matter ($PM_{2.5}$) in China. Atmos. Chem. Phys. 22, 11845–11866.
Liu, A., Yi, J., Ding, X., Deng, J., Wu, D., Huo, Y., et al., 2022a. An online technology for effectively monitoring inorganic condensable particulate matter emitted from industrial plants. J. Hazard. Mater. 428, 128221.
Liu, S., Wu, Y., Xu, Z., Lu, S., Li, X., 2022b. Study on characteristics of organic components in condensable particulate matter before and after wet flue gas desulfurization system of coal-fired power plants. Chemosphere 294, 133668.
Lu, C., Dat, N., Lien, C., Chi, K., Chang, M.B., 2019. Characteristics of fine particulate matter and polycyclic aromatic hydrocarbons emitted from coal combustion processes. Energy Fuel 33, 10247–10254.
Lu, S., Wu, Y., Chen, T., Song, J., Xu, Z., Tang, M., et al., 2020. Influence of the combination system of wet flue gas desulfurization and a wet electrostatic precipitator on the distribution of polycyclic aromatic hydrocarbons in flue gas from a coal-fired industrial plant. Energy Fuel 34, 5707–5714.
Morino, Y., Chatani, S., Tanabe, K., Fujitani, Y., Morikawa, T., Takahashi, K., et al., 2018. Contributions of condensable particulate matter to atmospheric organic aerosol over Japan. Environ. Sci. Technol. 52, 8456–8466.
Morino, Y., Chatani, S., Fujitani, Y., Tanabe, K., Murphy, B., Jathar, S., et al., 2022. Emissions of condensable organic aerosols from stationary combustion sources over Japan. Atmos. Environ. 289, 119319.
Murphy, B., Woody, M., Jimenez, J., Carlton, A., Hayes, P., Liu, S., et al., 2017. Semivolatile POA and parameterized total combustion SOA in CMAQv5.2: impacts on source strength and partitioning. Atmos. Chem. Phys. 17, 11107–11133.
Pham, T., Manomaiphiboon, K., Vongmahadlek, C., 2008. Development of an inventory and temporal allocation profiles of emissions from power plants and industrial facilities in Thailand. Sci. Total Environ. 397, 103–118.
Peng, Y., Shi, N., Wang, J., Wang, T., Pan, W., 2021. Mercury speciation and size-specific distribution in filterable and condensable particulate matter from coal combustion. Sci. Total Environ. 787, 147597.
Pye, H., Murphy, B., Xu, L., Ng, N., Carlton, A., Guo, H., et al., 2017. On the implications of aerosol liquid water and phase separation for organic aerosol mass. Atmos. Chem. Phys. 17, 343–369.
Sha, Q., Zhu, M., Huang, H., Wang, Y., Huang, Z., Zhang, X., et al., 2021. A newly integrated dataset of volatile organic compounds (VOCs) source profiles and implications for the future development of VOCs profiles in China. Sci. Total Environ. 793, 148348.
Shen, Z., Li, G., Liu, Z., et al., 2021. Optimal design and application of condensable particulate matter sampling system. Chin. J. Environ. Eng. 15, 3262–3269 (in Chinese).
Song, J., Lu, S., Wu, Y., Zhou, C., Li, X., Li, J., 2020. Migration and distribution characteristics of organic and inorganic fractions in condensable particulate matter emitted from an ultralow emission coal-fired power plant. Chemosphere 243, 125346.
Statistical Review of World Energy (SRWE), 2022. BP Statistical Review of World Energy in 2022. 71st edition. . https://www.bp.com/en/global/corporate/energy-economics/statistical-review-of-world-energy.html.
United States Environmental Protection Agency (US EPA), 2016. Method 202 Dry Impinger Method For Determining Condensable Particulate Emissions From Stationary Sources. U.S. EPA, Washington, D.C.
United States Environmental Protection Agency(US EPA), 2020. CMAQ (Version 5.4) [Software]. https://doi.org/10.5281/zenodo.4081737 Available from.
United States Environmental Protection Agency (US EPA), .. AP-42 (fifth Ed.): Compilation of Air Emissions Factors, Volume I, (Chapter 1): External Combustion Sources. https://www3.epa.gov/ttn/chief/ap42/ch01/final/c01s01.pdf. (Accessed 15 November 2021).
Wang, K., Yang, L., Li, J., Sheng, Z., He, Q., Wu, K., 2020a. Characteristics of condensable particulate matter before and after wet flue gas desulfurization and wet electrostatic precipitator from ultra-low emission coal-fired power plants in China. Fuel 278, 118206.
Wang, G., Deng, J., Zhang, Y., Li, Y., Ma, Z., Hao, J., et al., 2020b. Evaluating airborne condensable particulate matter measurement methods in typical stationary sources in China. Environ. Sci. Technol. 54, 1363–1371.
Wang, K., Gao, J., Liu, K., Tong, Y., Dan, M., Zhang, X., et al., 2022. Unit-based emissions and environmental impacts of industrial condensable particulate matter in China in 2020. Chemosphere 303, 134759.
Wu, B., Bai, X., Liu, W., Lin, S., Liu, S., Luo, L., Guo, Z., et al., 2020. Non-negligible stack emissions of noncriteria air pollutants from coal-fired power plants in China: condensable particulate matter and sulfur trioxide. Environ. Sci. Technol. 54, 6540–6550.
Wu, Y., Xu, Z., Liu, S., Tang, M., Lu, S., 2021a. Emission characteristics of PM2.5 and components of condensable particulate matter from coal-fired industrial plants. Sci. Total Environ. 796, 148782.
Wu, Y., Xu, Z., Liu, S., Tang, M., Lu, S., 2021b. Emission of organic components and distribution characteristics of PAHs in condensable particulate matter from coal-fired power and industrial plants. J. Energy Inst. 97, 109–116.
Wu, Y., Xu, Z., Huang, X., Liu, S., Tang, M., Lu, S., 2022a. A typical 300 MW ultralow emission coal-fired power plant: source, distribution, emission, and control of polycyclic aromatic hydrocarbons. Fuel 326, 123052.
Wu, Y., Xu, Z., Liu, S., Tang, M., Lu, S., 2022b. Effects of the changes of load and flue gas temperature on the emission of particulate matter from the coal-fired unit. Aerosol Air Qual. Res. 22, 210268.
Yang, H., Lee, K., Hsieh, Y., Luo, S., Huang, R., 2015. Emission characteristics and chemical compositions of both filterable and condensable fine particulate from steel plants. Aerosol Air Qual. Res. 15, 1672–1680.
Yang, H., Arafath, S., Lee, K., Hsieh, Y., Han, Y., 2018. Chemical characteristics of filterable and condensable PM2.5 emissions from industrial boilers with five different fuels. Fuel 232, 415–422.
Yang, F., Li, Z., Liu, H., Feng, P., Tan, H., Zhang, S., et al., 2021. Emission characteristics of condensable particulate matter and sulfur trioxide from coal-fired power plants. J. Energy Inst. 94, 146–156.
Yang, Y., Su, Q., Zheng, C., Zhang, Y., Wang, Y., Guo, D., et al., 2022. Emission characteristics of filterable particulate matter and condensable particulate matter from coal-fired power plants. Case Stud. Therm. Eng. 35, 102145.
Yuan, C., Wang, Z., Cheng, H., Liang, S., Hu, Y., Dong, X., et al., 2021. Characteristics of water-soluble ions in condensable particulate matter emitted from stationary sources in Wuhan. Fuel 295, 120626.
Yuan, C., Liang, S., Cheng, H., Xu, R., Su, S., Yao, Z., et al., 2022a. Assessing the dry impinger method for condensable particulate matter from ultra-low emission coal-fired power plant measurement. Sci. Total Environ. 834, 155002.
Yuan, C., Su, S., Xu, R., Liang, S., Cheng, H., Yao, Z., et al., 2022b. Effect of wet flue gas desulfurization on the concentrations and component profiles of condensable particulate matter from ultralow emission coal-fired power plants. Atmos. Pollut. Res. 13, 101376.
Zhai, Y., Liu, X., Han, J., Zou, Y., Huang, Y., Wang, H., et al., 2022. Study on the removal characteristics of different air pollution control devices for condensable particulate matter in coal-fired power plants. Environ. Sci. Pollut. Res. Int. 29, 34714–34724.
Zhang, Z., Li, Y., Zhang, X., Zhang, H., Wang, L., 2021. Review of hazardous materials in condensable particulate matter. Fuel Process. Technol. 220, 106892.
Zheng, C., Hong, Y., Liu, S., Yang, Z., Chang, Q., Zhang, Y., et al., 2018. Removal and emission characteristics of condensable particulate matter in an ultralow emission power plant. Energy Fuel 32, 10586–10594.